Journal of Sound and Vibration (1999) **227**(1), 85–103
Article No. jsvi.1999.2329, available online at http://www.idealibrary.com on IDEAL®

THE EFFECT OF BLADE CRACK ON MODE LOCALIZATION IN ROTATING BLADED DISKS

J. H. KUANG AND B. W. HUANG

Department of Mechanical Engineering, National Sun Yat-Sen University, Kaohsiung, Taiwan, R.O.C.

(*Received* 2 *January* 1998, *and in final form* 12 *April* 1999)

The effects of blade crack on mode localization in rotating bladed disks are investigated in this study. A disk consisting of periodic shrouded blades is used to simulate the bladed disk of a turbo-rotor. Blades on the disk are approximated as Euler–Bernoulli beams. A crack in the blade is regarded as a local disorder of the system. This local disorder might introduce the so-called mode localization phenomenon in this mistuned system. The Galerkin method is employed to derive the equation of motion of the mistuned system, with the blade crack. The effects of position, depth of crack and rotating speed on the localization phenomenon in the rotating blade-disk system are studied. Numerical results indicate that the blade crack may be one of the reasons for the occurrence of the localization phenomenon in the rotating bladed disk.

1. INTRODUCTION

The dynamic analysis of repetitious engineering structures is greatly simplified by assuming perfect periodicity. Unfortunately, this mathematical idealization is invalid due to unavoidable manufacturing and material defects. Due to manufacturing flows or cyclic fatigue during operation, cracks frequently appear in the rotating machinery [1, 2]. A blade crack may cause local change in the flexibility, i.e., structural irregularity which may change the dynamic behavior of the structure. As noted by several investigators [1, 9], the existence of a local defect in the coupled periodic system may introduce the so-called vibration localization phenomenon. However, these studies have not focused on the investigation of mode localization. Most types of crack are surface cracks in the rotating machinery, but it is difficult to emphasize on fracture mechanics in this model. To make the analysis even easier, the investigation of a two-dimensional problem using a model of a crack extends over the entire chord, is necessary. Krawczuk *et al.* [3–9] have studied the vibrational behavior for the blade, beam and rotor with a crack by the two-dimensional crack model. In this study, the crack blade is still modelled as a two-dimensional model, i.e., a two-span beam model [9].

The localization phenomenon is known to occur in coupled periodic structures under certain circumstances by local structural or material irregularities. Such localization may in turn localize the vibrational modes and thereby confine the

0022-460X/99/410085 + 19 $30.00/0

vibrational energy. Recently, a number of studies have been conducted to investigate mode localization in periodic structures [10–14]. Studies on normal mode localization in nearly periodic system in one, two and three dimensions were published by Cai *et al.* [15, 16]. Different models and parameter values used in the above analyses have, however yielded different and even conflicting conclusions.

The localization phenomenon may occur in a rotating bladed disk under certain circumstances, *such as structural or material irregularity*. The natural frequencies or mode shapes of the mistuned system can be seriously affected by such local irregularity. The amplitudes of individual defected blades may in turn be seriously excited. The localized vibrations further increase the amplitudes and stresses locally. The shrouded bladed disk of a turbo-rotor can be regarded as a periodic system if all the blades are assembled periodically. The dynamic behavior of such a shrouded blade-disk system has been studied by Cottney and Ewisn [17], whereas the fundamental aspects of mode localization in mistuned turbo-machinery rotors have been studied by Bendisksen *et al.* [18–21]. More recent studies by Cha and Pierre *et al.* [22–25] have dealt with vibrational localization in the mistuned system with a multi-mode subsystem.

Most of the studies on mode localization are limited to stationary structures, with assumed structural and material irregularity. Only a few studies on the effects of crack and rotation on localization in a shrouded bladed disk have been conducted.

The individual blades of the shrouded blade-disk are approximated as Euler–Bernoulli beams, and a two-span beam with a torsional spring is used in modelling the cracked blade. The shrouded effect, which is regarded as a massless spring effect, is considered in order to introduce the constraint between the blades. The effects of crack size, crack position and rotation speed on mode localization in the shrouded blade disk have been investigated in this study.

2. EQUATIONS OF MOTION

The periodic shrouded blade structure is shown in Figure 1, consisting of a rigid hub and a cyclic assembly of N coupled blades. Each blade is coupled with the adjacent one through a shroud. A massless spring k_s is assumed to model the function of this shroud. The length of the cantilever beam is $L = R_o - R_h$, and every blade is coupled by a spring k_s to the adjacent one at position R_c. The notation $v_s(r, t)$ denotes the transverse flexible deflection of the sth blade as a constant rotating speed Ω.

The moment of inertia and the cross-sectional area of the sth blade are denoted as I_s and A_s respectively, while the Young's modulus of the blade is denoted as E.

2.1. BLADES WITHOUT CRACK

According to Kuang and Huang [26], the effect of coriolis force on the mode localization phenomenon in a turbo disk system is not significant. By neglecting the coriolis force and *the vibration* in the radial direction, the kinetic energy of the sth

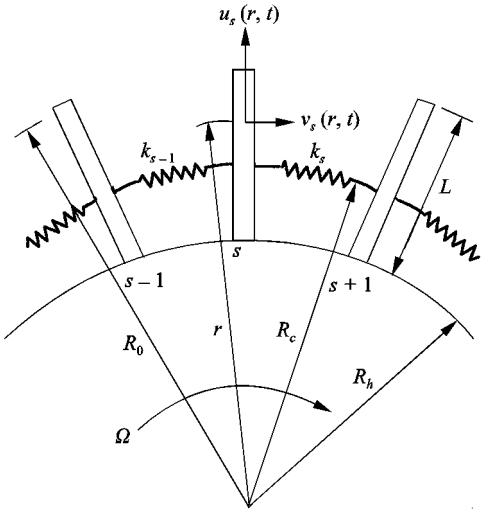

Figure 1. Geometry of the rotating bladed disk.

blade is given by

$$T_s = \frac{\rho A_s}{2} \int_{R_h}^{R_o} \left\{ \left[\frac{\partial v_s(r, t)}{\partial t} \right]^2 + [\Omega v_s(r, t)]^2 \right\} \mathrm{d}r, \tag{1}$$

where the subscript s denotes the blade number of the disk. The corresponding strain energy of the sth blade is

$$U_s = \frac{1}{2} \int_{R_h}^{R_o} EI_s \left[\frac{\partial^2 v_s(r, t)}{\partial r^2} \right]^2 \mathrm{d}r + \frac{1}{4} \rho A_s \Omega^2 \int_{R_h}^{R_o} \left[(R_h + L)^2 - r^2 \right] \left(\frac{\partial v_s(r, t)}{\partial r} \right)^2 \mathrm{d}r$$
$$+ \frac{1}{2} k_s [v_{s+1}(R_c, t) - v_s(R_c, t)]^2. \tag{2}$$

By applying Hamilton's principle, the equation of motion of the sth blade in the transverse direction can be obtained as

$$\frac{\partial}{\partial t} \left[\frac{\partial v_s(r, t)}{\partial t} \right] + \frac{EI_s}{\rho A_s} \frac{\partial^2}{\partial r^2} \left(\frac{\partial^2 v_s(r, t)}{\partial r^2} \right)$$
$$+ \Omega^2 \left\{ r \frac{\partial v_s(r, t)}{\partial r} - v_s(r, t) - \frac{1}{2} [(R_h + L)^2 - r^2] \frac{\partial}{\partial r} \left(\frac{\partial v_s(r, t)}{\partial r} \right) \right\}$$
$$+ (k_s + k_{s-1}) v_s \delta(r - R_c) - k_s v_{s+1} \delta(r - R_c) - k_{s-1} v_{s-1} \delta(r - R_c) = 0$$
$$\text{for } s = 1, 2, \ldots, N. \tag{3}$$

For simplifying the notations, a number of non-dimensional parameters are defined as

$$\bar{r} = \frac{r - R_h}{L} \quad \text{and} \quad \bar{r} = 0 \rightarrow 1, \tag{4}$$

$$\bar{v}_s(\bar{r}, t) = \frac{v_s(\bar{r}, t)}{L}, \tag{5}$$

$$\bar{\Omega} = \Omega \Big/ \sqrt{\frac{EI}{\rho A L^4}}, \tag{6}$$

$$\bar{R}_c = \frac{R_c - R_h}{L} \quad \text{and} \quad \frac{R_h}{L} = \frac{1}{2}, \tag{7}$$

$$\bar{\beta} = \frac{k_s L^3}{EI_s}. \tag{8}$$

By substituting these dimensionless variables into the equation of motion of the sth blade, it yields

$$\begin{aligned} &\frac{\partial^2 \bar{v}_s}{\partial t^2} + \frac{EI}{\rho A_s L^4} \left\{ \frac{\partial^2}{\partial \bar{r}^2} \left(\frac{\partial^2 \bar{v}_s}{\partial \bar{r}^2} \right) \right. \\ &\quad \left. + \bar{\Omega}^2 \left\{ \bar{r} \frac{\partial \bar{v}_s}{\partial \bar{r}} - \bar{v}_s - \frac{1}{2} \left[\left(\frac{R_h}{L} + 1 \right)^2 - \left(\bar{r} + \frac{R_h}{L} \right)^2 \right] \frac{\partial}{\partial \bar{r}} \left(\frac{\partial \bar{v}_s}{\partial \bar{r}} \right) \right\} \right\} \\ &\quad + (\bar{\beta}_s + \bar{\beta}_{s-1}) \bar{v}_s \delta(\bar{r} - \bar{R}_c) - \bar{\beta}_s \bar{v}_{s+1} \delta(\bar{r} - \bar{R}_c) - \bar{\beta}_{s-1} \bar{v}_{s-1} \delta(\bar{r} - \bar{R}_c) = 0 \end{aligned} \tag{9}$$

for $s = 1, 2, \ldots, N$, with the boundary conditions

$$\bar{v}_s(0, t) = 0, \tag{10}$$

$$\frac{\partial \bar{v}_s(0, t)}{\partial \bar{r}} = 0, \tag{11}$$

$$\frac{\partial^2 \bar{v}_s(1, t)}{\partial \bar{r}^2} = 0, \tag{12}$$

$$\frac{\partial}{\partial \bar{r}} \left[\frac{\partial^2 \bar{v}_s(1, t)}{\partial \bar{r}^2} \right] = 0. \tag{13}$$

The solution of the above eigenvalue problem can be expressed as

$$\bar{v}_s(\bar{r}, t) = \sum_{i=1}^{m} q_i^s(t) \psi_i^s(\bar{r}), \tag{14}$$

where $\psi_i^s(\bar{r})$ is the comparison function of equation (9) and $q_i^s(t)$ the coefficient, which is to be determined. For simplicity, three exact bending modes of the clamped cantilever beam $\psi_i^s(\bar{r})$ are considered in this article. They are

$$\psi_i^s(\bar{r}) = (\cosh \lambda_i r^- - \cos \lambda_i \bar{r}) - \frac{\cos \lambda_i + \cosh \lambda_i}{\sin \lambda_i + \sinh \lambda_i} (\sinh \lambda_i \bar{r} - \sin \lambda_i \bar{r})$$

$$\text{for } i = 1, 2, \ldots, m, \tag{15}$$

The coefficients λ_i are the roots of

$$\cos \lambda_i \bar{r} \cosh \lambda_i \bar{r} + 1 = 0. \tag{16}$$

Using Galerkin method, the equation of motion of the sth blade can be derived in matrix form as

$$[m]_s\{\ddot{q}\}_s + \frac{EI}{\rho A_s L^4}\{[[k]_s + [\Lambda]_s + \bar{\beta}_s\{\psi(\bar{R}_c)\}_s\{\psi(\bar{R}_c)\}_s^{\mathrm{T}} + \bar{\beta}_{s-1}\{\psi(\bar{R}_c)\}_s\{\psi(\bar{R}_c)\}_s^{\mathrm{T}}]\{q\}_s - \bar{\beta}_{s-1}\{\psi(\bar{R}_c)\}_s\{\psi(\bar{R}_c)\}_{s-1}^{\mathrm{T}}]\{q\}_{s-1} - \bar{\beta}_s\{\psi(\bar{R}_c)\}_s\{\psi(\bar{R}_c)\}_{s+1}^{\mathrm{T}}\{q\}_{s+1}\} = 0 \quad (17)$$

for $s = 1, 2, \ldots, N$ and $\{\psi(r)\}_s = [\psi_1^s(r), \psi_2^s(r), \ldots, \psi_m^s(r)]^{\mathrm{T}}$.

Due to the cyclic arrangement of blades

$$\{q\}_{N+1} = \{q\}_1,$$

where the elements $(m)_{ij}^s$, $(k)_{ij}^s$ and $(\Lambda)_{ij}^s$ are given as

$$(m)_{ij}^s = (m)_{ji}^s = \int_0^1 \psi_i^s(\bar{r})\,\psi_j^s(\bar{r})\,\mathrm{d}\bar{r}, \quad (18)$$

$$(k)_{ij}^s = (k)_{ji}^s = \int_0^1 \frac{\mathrm{d}^2\psi_i^s(\bar{r})}{\mathrm{d}\bar{r}^2}\frac{\mathrm{d}^2\psi_j^s(\bar{r})}{\mathrm{d}\bar{r}^2}\,\mathrm{d}\bar{r}, \quad (19)$$

$$(\Lambda)_{ij}^2 = \bar{\Omega}^2\int_0^1 \psi_i^s(\bar{r})\left\{\left(\bar{r} + \frac{R_h}{L}\right)\frac{\mathrm{d}\psi_j^s(\bar{r})}{\mathrm{d}\bar{r}} - \psi_j^s(\bar{r}), - \frac{1}{2}\left[\left(\frac{R_h}{L} + 1\right)^2 - \left(\bar{r} + \frac{R_h}{L}\right)^2\right]\frac{\partial}{\partial\bar{r}}\left(\frac{\mathrm{d}\psi_j^s(\bar{r})}{\mathrm{d}r}\right)\right\}\mathrm{d}\bar{r}. \quad (20)$$

2.2. BLADE WITH A CRACK

Considering a crack on the ξth blade of this system, it may be regarded as a mistuned system. The response of the ξth cracked blade can be expressed as

$$\bar{v}_\xi(\bar{r}, t) = \sum_{i=1}^{m} q_i^\xi(t)\,\psi_i^\xi(\bar{r}), \quad (21)$$

where $\psi_i^\xi(\bar{r})$ are comparison functions of equation of motion of the cracked blade. The $q_i^\xi(t)$ are the coefficients to be determined. For simplicity, only three bending modes are considered in this study, and they are calculated from the cracked beam model. The cracked blade, as shown in Figure 2, is modelled as a two-span beam coupled with a torsional spring. This cracked beam model has been studied by Rizos and Asprogathos [9]. The notation L_c denotes the position of the crack, while the depth of the crack is a. The flexibility G caused by the crack with depth a can be derived from Broke's approximation [27] as

$$\frac{(1-\mu^2)K_I^2}{E} = \frac{(Pb)^2}{2b}\frac{\mathrm{d}G}{\mathrm{d}a}, \quad (22)$$

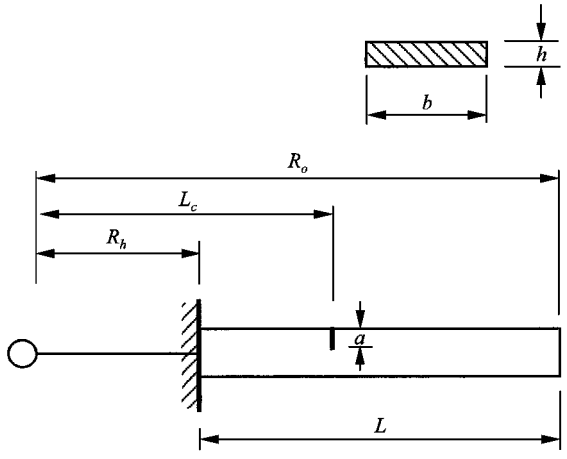

Figure 2. Geometry of the cracked blade.

where K_I is the stress intensity factor under mode I loading, μ the Poisson Ratio, b the width of the blade, h the height of the blade, P_b the bending moment at the crack, and G the flexibility of the blade.

The magnitude of stress intensity factor can be derived from Tada's formula [28] as

$$K_I = \frac{6P_b}{gh^2}\sqrt{\pi\gamma h}\,F_I(\gamma), \tag{23}$$

where

$$F_I(\gamma) = \sqrt{\frac{2}{\pi\gamma}\tan\left(\frac{\pi\gamma}{2}\right)}\,\frac{0{\cdot}923 + 0{\cdot}199\,[1-\sin(\pi\gamma/2)]^4}{\cos(\pi\gamma/2)}, \tag{24}$$

$$\gamma = \frac{a}{h}. \tag{25}$$

By substituting the stress intensity factor K_I in equation (22), it leads to

$$G = \frac{6(1-\mu^2)h}{EI}\,Q(\gamma) \tag{26}$$

and

$$Q(\gamma) = \int_0^{\gamma} \pi\gamma\,F_I^2(\gamma)\,\mathrm{d}\gamma.$$

Since

$$k_T = \frac{1}{G} \tag{27}$$

the bending stiffness k_T of the cracked section of a blade can be expressed as

$$k_T = \frac{EI}{6(1-\mu^2)hQ(\gamma)}. \tag{28}$$

The corresponding kinetic energy of the cracked blade is

$$T_\xi = \frac{\rho A_\xi}{2}\left(\int_{R_h}^{L_c}\left(\frac{\partial v_{\xi 1}(r,t)}{\partial t}\right)^2 \mathrm{d}r + \int_{L_c}^{R_o}\left(\frac{\partial v_{\xi 2}(r,t)}{\partial t}\right)^2 \mathrm{d}r\right). \tag{29}$$

The strain energy of the cracked blade can thus be found as

$$U_\xi = \frac{1}{2}\int_{R_h}^{L_c} EI_\xi\left[\frac{\partial^2 v_{\xi 1}(r,t)}{\partial r^2}\right]^2 \mathrm{d}r + \frac{1}{2}\int_{L_c}^{R_o} EI_\xi\left[\frac{\partial^2 v_{\xi 2}(r,t)}{\partial r^2}\right]^2 \mathrm{d}r + \frac{1}{2}k_T\left[\frac{\partial v_{\xi 1}}{\partial r}(L_c,t) - \frac{\partial v_{\xi 2}}{\partial r}(L_c,t)\right]^2. \tag{30}$$

In this case, the equation of motion of the cracked blade can be derived as

$$\frac{\partial^2 \bar{v}_{\xi 1}}{\partial t^2} + \frac{EI_\xi}{\rho A_\xi L^4}\left\{\frac{\partial^2}{\partial \bar{r}^2}\left(\frac{\partial^2 \bar{v}_{\xi 1}}{\partial \bar{r}^2}\right)\right\} = 0 \quad \text{for } \bar{r}\text{: 0 to } \bar{L}_c, \tag{31}$$

$$\frac{\partial^2 \bar{v}_{\xi 2}}{\partial t^2} + \frac{EI_\xi}{\rho A_\xi L^4}\left\{\frac{\partial^2}{\partial \bar{r}^2}\left(\frac{\partial^2 \bar{v}_{\xi 2}}{\partial \bar{r}^2}\right)\right\} = 0 \quad \text{for } \bar{r}\text{: } \bar{L}_c \text{ to } 1, \tag{32}$$

where

$$\bar{L}_c = \frac{L_c - R_h}{L}. \tag{33}$$

The boundary conditions of this cracked blade are

$$\bar{v}_{\xi 1}(0,t) = 0, \tag{34}$$

$$\frac{\partial \bar{v}_{\xi 1}}{\partial \bar{r}}(0,t) = 0, \tag{35}$$

$$\bar{v}_{\xi 1}(\bar{L}_c,t) = \bar{v}_{\xi 2}(\bar{L}_c,t), \tag{36}$$

$$\frac{\partial^2 \bar{v}_{\xi 1}}{\partial \bar{r}^2}(\bar{L}_c,t) = \frac{\partial^2 \bar{v}_{\xi 2}}{\partial \bar{r}^2}(\bar{L}_c,t), \tag{37}$$

$$\frac{\partial^3 \bar{v}_{\xi 1}}{\partial \bar{r}^3}(\bar{L}_c,t) = \frac{\partial^3 \bar{v}_{\xi 2}}{\partial \bar{r}^3}(\bar{L}_c,t), \tag{38}$$

$$\frac{\partial \bar{v}_{\xi 1}}{\partial \bar{r}}(\bar{L}_c,t) + \frac{EI_\xi}{k_T L}\frac{\partial^2 \bar{v}_{\xi 1}}{\partial \bar{r}^2}(\bar{L}_c,t) = \frac{\partial \bar{v}_{\xi 2}}{\partial \bar{r}}(\bar{L}_c,t), \tag{39}$$

$$\frac{\partial^2 \bar{v}_{\xi 2}}{\partial \bar{r}^2}(l,t) = 0, \tag{40}$$

$$\frac{\partial^3 \bar{v}_{\xi 2}}{\partial \bar{r}^3}(l,t) = 0. \tag{41}$$

The solutions of such a two-span beam with a torsional spring can be assumed to be as

$$\bar{v}_{\xi 1}(\bar{r}, t) = \sum_{i=1}^{m} q_i^{\xi}(t)\, \phi_i^{\xi 1}(\bar{r}), \tag{42}$$

$$\bar{v}_{\xi 2}(\bar{r}, t) = \sum_{i=1}^{m} q_i^{\xi}(t)\, \phi_i^{\xi 2}(\bar{r}), \tag{43}$$

where

$$\phi_i^{\xi 1}(\bar{r}) = A_1 \sin(\mu_i \bar{r}) + A_2 \cos(\mu_i \bar{r}) + A_3 \sinh(\mu_i \bar{r}) + A_4 \cosh(\mu_i \bar{r}), \tag{44}$$

$$\phi_i^{\xi 2}(\bar{r}) = B_1 \sin(\mu_i \bar{r}) + B_2 \cos(\mu_i \bar{r}) + B_3 \sinh(\mu_i \bar{r}) + B_4 \cosh(\mu_i \bar{r}). \tag{45}$$

Three modes, i.e., $m = 3$ are assumed. The coefficients of functions $\phi_i^{\xi 1}(\bar{r})$ and $\phi_i^{\xi 2}(\bar{r})$ can be obtained by substituting equations (44) and (45) in the above boundary conditions. Table 1 lists coefficients for the blade with a crack at the root. The coefficients for the blade with a crack at different positions, i.e., $\bar{L}_c = 0{\cdot}2$ and $0{\cdot}4$ are presented in Table 2. The comparison functions of the whole cracked blade can thus be expressed as

$$\psi_i^{\xi}(\bar{r}) = \phi_i^{\xi 1}(\bar{r})\, u(\bar{r}) - \phi_i^{\xi 1}(\bar{r})\, u(\bar{r} - \bar{L}_c) + \phi_i^{\xi 2}(\bar{r})\, u(\bar{r} - \bar{L}_c), \tag{46}$$

where $u(\bar{r})$ is a unit step function.

TABLE 1

The magnitude of coefficients for the blade with a crack at the root

(a) $\bar{L}_c = 0{\cdot}0$, $\gamma = 0{\cdot}01$

	B_1	B_2	B_3	B_4	μ_i
$i = 1$	1·00010	− 1·36214	− 0·99987	1·36214	1·8750
$i = 2$	1·00019	− 0·98167	− 0·99981	0·981678	4·6939
$i = 3$	1·00024	− 1·00037	− 0·99973	1·00051	7·8546

(b) $\bar{L}_c = 0{\cdot}0$, $\gamma = 0{\cdot}05$

	B_1	B_2	B_3	B_4	μ_i
$i = 1$	1·00245	− 1·36042	− 0·99755	1·36042	1·8733
$i = 2$	1·00441	− 0·97737	− 0·99559	0·977379	4·6896
$i = 3$	1·00745	− 0·99328	− 0·99254	0·993322	7·8473

(c) $\bar{L}_c = 0{\cdot}0$, $\gamma = 0{\cdot}10$

	B_1	B_2	B_3	B_4	μ_i
$i = 1$	1·00929	− 1·35542	− 0·99070	1·35542	1·8683
$i = 2$	1·01656	− 0·96499	− 0·98343	0·964995	4·6772
$i = 3$	1·02795	− 0·97302	− 0·97211	0·972909	7·8269

Note: Only B_1, B_2, B_3, B_4, as the crack at the root of blade.

TABLE 2

The magnitude of coefficients for the blade with a crack at different locations

(a) $\bar{L}_c = 0{\cdot}2$, $\gamma = 0{\cdot}10$

	A_1	A_2	A_3	A_4	μ_i
$i = 1$	1·0000	− 1·3597	− 1·0000	1·3397	1·8715
$i = 2$	1·0000	− 0·98138	− 1·0000	0·98138	4·6940
$i = 3$	1·0000	− 1·01206	− 1·0000	1·01206	7·8327
	B_1	B_2	B_3	B_4	μ_i
$i = 1$	1·00631	− 1·36217	− 0·99274	1·35710	1·8715
$i = 2$	1·00071	− 0·98234	− 1·99822	0·98007	4·6940
$i = 3$	1·02197	− 0·97863	− 1·24493	1·24573	7·8327

(b) $\bar{L}_c = 0{\cdot}4$, $\gamma = 0{\cdot}10$

	A_1	A_2	A_3	A_4	μ_i
$i = 1$	1·0000	− 1·36154	− 1·0000	1·36154	1·8736
$i = 2$	1·0000	− 0·98337	− 1·0000	0·98337	4·6882
$i = 3$	1·0000	− 1·00139	− 1·0000	1·00139	7·8488
	B_1	B_2	B_3	B_4	μ_i
$i = 1$	1·00316	− 1·36449	− 0·99441	1·35800	1·8736
$i = 2$	1·00280	− 0·97374	− 1·03175	0·01356	4·6882
$i = 3$	1·01379	− 1·00244	− 1·14455	1·14534	7·8488

By substituting equations (42) and (43) into equations (31) and (32), the equation of motion of the cracked blade can be obtained in the matrix form as

$$[m]_\xi \{\ddot{q}\}_\xi + \frac{EI_\xi}{\rho A_\xi L^4} \{[[k]_\xi + [\Lambda]_\xi + \bar{\beta}_\xi \{\psi(\bar{R}_c)\}_\xi \{\psi(\bar{R}_c)\}_\xi^{\mathrm{T}} + \bar{\beta}_{\xi-1} \{\psi(\bar{R}_c)\}_\xi \{\psi(\bar{R}_c)\}_\xi^{\mathrm{T}}] \{q\}_\xi - \bar{\beta}_{\xi-1} \{\psi(\bar{R}_c)\}_\xi \{\psi(\bar{R}_c)\}_{\xi-1}^{\mathrm{T}} \{q\}_{\xi-1} - \bar{\beta}_\xi \{\psi(\bar{R}_c)\}_\xi \{\psi(\bar{R}_c)\}_{\xi+1}^{\mathrm{T}} \{q\}_{\xi+1}\} = 0 \quad (47)$$

with

$$(m)_{ij}^\xi = (m)_{ji}^\xi = \int_0^1 \psi_i^\xi(\bar{r})\, \psi_j^\xi(\bar{r})\, \mathrm{d}\bar{r}, \quad (48)$$

$$(k)_{ij}^\xi = (k)_{ji}^\xi = \int_0^1 \frac{\mathrm{d}^2 \psi_i^\xi(\bar{r})}{\mathrm{d}\bar{r}^2} \frac{\mathrm{d}^2 \psi_j^\xi(\bar{r})}{\mathrm{d}\bar{r}^2}\, \mathrm{d}\bar{r}, \quad (49)$$

$$(\Lambda)_{ij}^2 = \bar{\Omega}^2 \int_0^1 \psi_i^{\xi}(\bar{r}) \left\{ \left(\bar{r} + \frac{R_h}{L} \right) \frac{\mathrm{d}\psi_j^{\xi}(\bar{r})}{\mathrm{d}\bar{r}} - \psi_j^{\xi}(\bar{r}), \right.$$
$$\left. - \frac{1}{2} \left[\left(\frac{R_h}{L} + 1 \right)^2 - \left(\bar{r} + \frac{R_h}{L} \right)^2 \right] \frac{\partial}{\partial \bar{r}} \left(\frac{\mathrm{d}\psi_j^{\xi}(\bar{r})}{\mathrm{d}\bar{r}} \right) \right\} \mathrm{d}\bar{r}. \tag{50}$$

2.3. EQUATION OF MOTION OF THE MISTUNED SYSTEM

For the sake of simplicity, the same comparison function is assumed for each individual blade, i.e., $\psi_j^s(\bar{r}) \equiv \psi_j(\bar{r})$. The equation of motion of the entire disk system can be expressed as

$$[M]\{\ddot{X}\} + [K]\{X\} = 0, \tag{51}$$

where the system mass matrix $[M]$ and the system stiffness matrix $[K]$ are

$$[M] = \begin{bmatrix} [m]_1 & 0 & 0 & . & 0 & 0 & 0 \\ 0 & [m]_2 & 0 & . & 0 & 0 & 0 \\ 0 & 0 & [m]_3 & . & 0 & 0 & 0 \\ . & . & . & . & . & . & . \\ 0 & 0 & 0 & . & [m]_{N-2} & 0 & 0 \\ 0 & 0 & 0 & . & 0 & [m]_{N-1} & 0 \\ 0 & 0 & 0 & . & 0 & 0 & [m]_N \end{bmatrix}, \tag{52}$$

$$[K] = \frac{EI}{\rho A L^4} \begin{bmatrix} [\bar{\alpha}]_1 & -\bar{\beta}_1[\Phi] & 0 & . & 0 & 0 & -\bar{\beta}_N[\Phi] \\ -\bar{\beta}_1[\Phi] & [\bar{\alpha}]_2 & -\bar{\beta}_2[\Phi] & . & 0 & 0 & 0 \\ 0 & -\bar{\beta}_2[\Phi] & [\bar{\alpha}]_3 & . & 0 & 0 & 0 \\ . & . & . & . & . & . & . \\ 0 & 0 & 0 & . & [\bar{\alpha}]_{N-2} & -\bar{\beta}_{N-2}[\Phi] & 0 \\ 0 & 0 & 0 & . & -\bar{\beta}_{N-2}[\Phi] & [\bar{\alpha}]_{N-1} & -\bar{\beta}_{N-1}[\Phi] \\ -\bar{\beta}_N[\Phi] & 0 & 0 & . & 0 & -\bar{\beta}_{N-1}[\Phi] & [\bar{\alpha}]_N \end{bmatrix}, \tag{53}$$

$$\{X\} = [\{q\}_1^{\mathrm{T}}, \{q\}_2^{\mathrm{T}}, \ldots, \{q\}_{N-1}^{\mathrm{T}}, \{q\}_N^{\mathrm{T}}]^{\mathrm{T}} \tag{54}$$

and

$$[\bar{\alpha}]_s = [k_s] + [\Lambda]_s + \bar{\beta}_s[\Phi] + \bar{\beta}_{s-1}[\Phi], \tag{55}$$

$$[\Phi] = \{\psi_i(\bar{R}_c)\}\{\psi_j(\bar{R}_c)\}^{\mathrm{T}}, \tag{56}$$

$$\bar{\beta}_0 = \bar{\beta}_N. \tag{57}$$

The non-dimensional frequency $\bar{\omega}_n$ of equation (51), i.e., the natural frequency of the mistuned system, is defined as

$$\bar{\omega}_n = \omega_n \Big/ \sqrt{\frac{EI}{\rho A L^4}} \quad \text{for } n = 1, 2, \ldots . \tag{58}$$

The lowest natural frequency of the tuned system without any rotational speed, i.e., $\bar{\omega}_1^* = 3{\cdot}516$, is used for reference in the following numerical analysis.

2.4. FORCE RESPONSE

Consider the blades to be excited by a uniformly distributed harmonic force $h_0 \cos \omega t$. The equation of motion of the sth blade can be rewritten in the matrix form as

$$[M]\{\ddot{X}\} + [K]\{X\} = \{F\} \cos \omega t, \tag{59}$$

where

$$\{F\} = [\{f\}_1^{\mathrm{T}}, \{f\}_2^{\mathrm{T}}, \ldots, \{f\}_{N-1}^{\mathrm{T}}, \{f\}_N^{\mathrm{T}}]^{\mathrm{T}}, \tag{60}$$

$$f_s = \int_0^1 \psi_s(\bar{r}) \bar{h}_0 \, \mathrm{d}r, \tag{61}$$

$$\bar{h}_0 = \frac{h_0}{\rho A_s}. \tag{62}$$

Let the dynamic response of the bladed-disk system be

$$\{X\} = [U]\{\eta(t)\}. \tag{63}$$

The modal matrix $[U]$ of the mistuned system is calculated from equation (51). With the initial condition as $\eta_i(0) = 0$, $\dot{\eta}_i(0) = 0$, the response of the system can be derived as

$$\eta_i(t) = \frac{\Gamma_i}{2\bar{\omega}_i} \left\{ \cos \bar{\omega} t \left[\frac{1 - \cos(\bar{\omega}_i + \bar{\omega}) t}{\bar{\omega}_i + \bar{\omega}} + \frac{1 - \cos(\bar{\omega}_i - \bar{\omega}) t}{\bar{\omega}_i - \bar{\omega}} \right] \right\}$$
$$+ \sin \bar{\omega} t \left\{ \frac{\sin(\bar{\omega}_i - \bar{\omega}) t}{\bar{\omega}_i - \bar{\omega}} - \frac{\sin(\bar{\omega}_i + \bar{\omega}) t}{\bar{\omega}_i + \bar{\omega}} \right\} \quad \text{for } \bar{\omega} \neq \bar{\omega}_i \tag{64}$$

with

$$\{\Gamma\} = [U]^{\mathrm{T}}\{F\}. \tag{65}$$

The corresponding resonant response can be written as

$$\eta_i(t) = \frac{\Gamma_s}{4\bar{\omega}_s^2} [\cos \bar{\omega}_s t (1 - \cos 2\bar{\omega}_s t) + \sin \bar{\omega}_s t (2\bar{\omega}_s t - \sin 2\bar{\omega}_s t)] \quad \text{for } \bar{\omega} = \bar{\omega}_s, \tag{66}$$

where $\bar{\omega}_s$ is one of the natural frequencies of system.

3. NUMERICAL RESULTS AND DISCUSSIONS

A rigid hub attached to 46 uniform blades is used to approximate the bladed disk. The existence of mode localization for a mistuned bladed disk system with a cracked blade is investigated. The effects of rotational speed of the disk, depth and location of the crack on mode localization have also been studied.

As the crack propagates on a blade, it may not only alter the dynamic behavior of this blade, but may also introduce the so-called mode localization phenomenon in

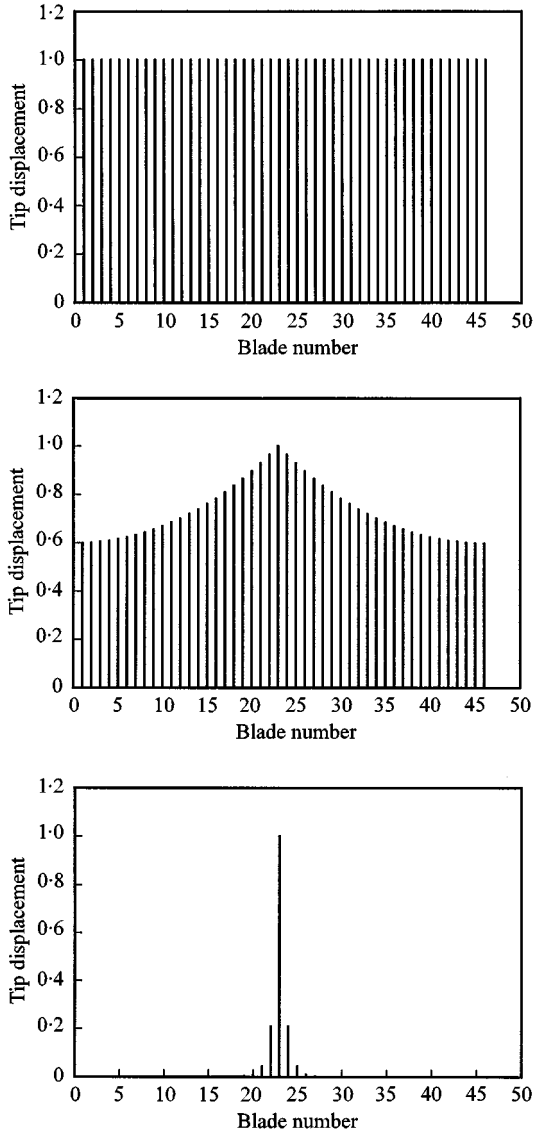

Figure 3. Tip displacements of the uncracked and cracked systems with different depths of crack (for the the 1st mode), $\bar{R}_c = 0{\cdot}5$, $\bar{L}_c = 0{\cdot}0$, $\bar{\beta} = 0{\cdot}2$, $\bar{\Omega}/\bar{\omega}_1^* = 0{\cdot}0$, $\bar{\omega}_1^* = 3{\cdot}516$: (a) system without crack $\gamma = 0{\cdot}0$ ($\bar{\omega}_1 = 3{\cdot}516$); (b) system with a crack $\gamma = 0{\cdot}01$ ($\bar{\omega}_1 = 3{\cdot}516$); (c) system with a crack $\gamma = 0{\cdot}1$ ($\bar{\omega}_1 = 3{\cdot}476$).

the whole mistuned system. In this numerical example, a crack is assumed on the 23rd blade.

3.1. FREE VIBRATION ANALYSIS

Figure 3(a) shows the tip vibration pattern of the tuned system at the lowest resonant frequency $\bar{\omega}_1^* = 3{\cdot}516$. The vibrational energy is uniformly distributed on the individual blades of the tuned system. The corresponding tip vibrational

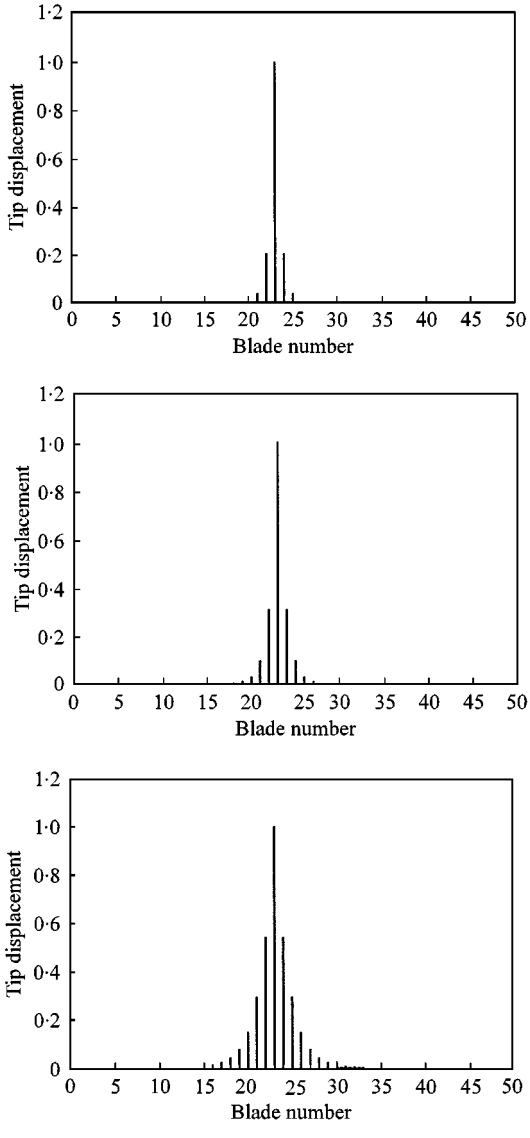

Figure 4. Tip displacements of the system with a crack at different locations (for the the 1st mode), $\bar{R}_c = 0{\cdot}5$, $\gamma = 0{\cdot}1$, $\bar{\beta} = 0{\cdot}2$, $\bar{\Omega}/\bar{\omega}_1^* = 0{\cdot}0$, $\bar{\omega}_1^* = 3{\cdot}516$: (a) system without crack at $\bar{L}_c = 0{\cdot}0$ ($\bar{\omega}_1 = 3{\cdot}476$); (b) system with a crack at $\bar{L}_c = 0{\cdot}2$ ($\bar{\omega}_1 = 3{\cdot}495$); (c) system with a crack at $\bar{L}_c = 0{\cdot}4$ ($\bar{\omega}_1 = 3{\cdot}511$).

patterns for the mistuned system, with different depths of crack, i.e., $\gamma = 0{\cdot}01$ and 0·1, are shown in Figures 3(b) and 3(c). These figures indicate that the vibrational energy is confined on the blades near the cracked blade of these two mistuned systems. It can also be observed that the localization pattern varies with the depth of the crack. Generally, the model localization phenomenon is enhanced with increase in the crack depth. The localization pattern may also be affected by location of the crack. The tip vibration pattern for different crack locations are shown in Figure 4(a)–4(c), which indicate that the

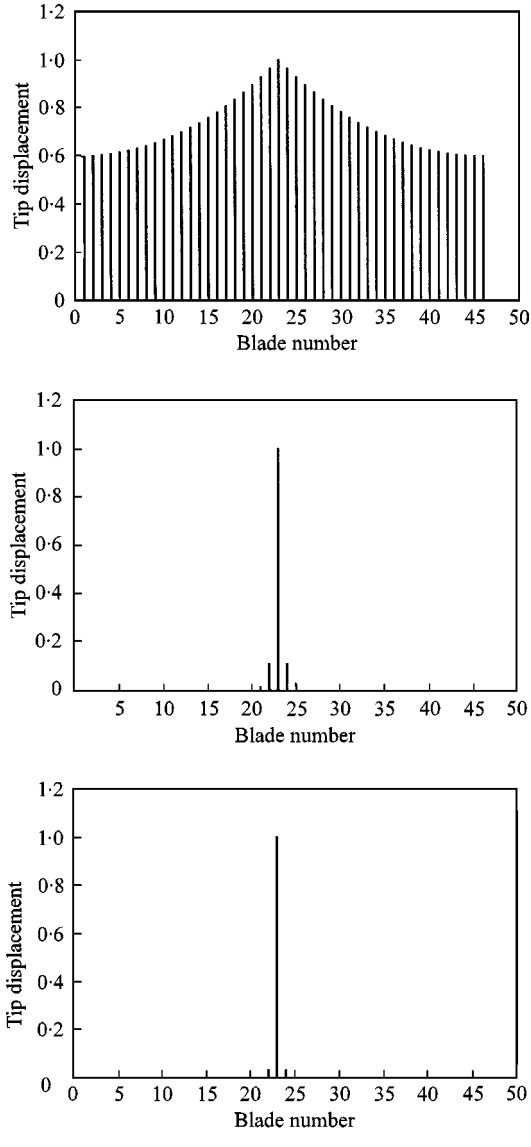

Figure 5. Tip displacements of the cracked system under different rotating speeds (for the 1st mode), $\gamma = 0{\cdot}01$, $\bar{L}_c = 0{\cdot}0$, $\bar{R}_c = 0{\cdot}5$, $\bar{\beta} = 0{\cdot}2$, $\bar{\omega}_1^* = 3{\cdot}516$: (a) crack system without speed $\bar{\Omega}/\bar{\omega}_1^* = 0{\cdot}0$ ($\bar{\omega}_1 = 3{\cdot}516$); (b) crack system at the speed $\bar{\Omega}/\bar{\omega}_1^* = 0{\cdot}25$ ($\bar{\omega}_1 = 3{\cdot}528$); (c) crack system at the speed $\bar{\Omega}/\bar{\omega}_1^* = 0{\cdot}5$ ($\bar{\omega}_1 = 3{\cdot}529$).

localization phenomenon is suppressed as the crack position is changed from $\bar{L}_c = 0{\cdot}0$ to $0{\cdot}4$.

Figures 5(a)–5(c) illustrate the effect of rotational speed Ω on mode localization in the mistuned system. These results appear to indicate that the confinement of vibrations may be strongly localized as the rotational speed is increased. In other words, mode localization phenomenon may be enhanced as the rotational speed is increased. The weak or strong localization phenomenon depends upon the magnitude of disorder and the modal coupling effect. Now, the strong modal coupling effect is studied in this investigation. Figure 6(a) shows the weak localization at the lower order mode $\bar{\omega}_1$ as the strong coupling stiffness at the blade tip. However, as above, the strong localization may appear at the higher order mode as shown in Figure 6(b).

3.2. FORCE RESPONSE

Consider that the blades of the system are excited by a uniformly distributed harmonic force with an excitation frequency $\bar{\omega}$. A significant resonant response of the cracked blade can be observed as the excitation frequency approaches the localization frequency, i.e., the lowest natural frequency of the mistuned system. Figure 7 shows the time response of the blades near the cracked blade, for excitation at the localization frequency $\bar{\omega} = \bar{\omega}_1 = 3{\cdot}529$.

Figure 8 shows the changes in frequency response of the 23rd blade with or without a crack located at the fixed end. There is only a single peak, $\bar{\omega} = \bar{\omega}_1 = 3{\cdot}516$, in the frequency spectra of the 23rd blade in the tuned system, which shows that every individual blade possesses the same frequency and mode. However, a group of peaks is observed for the corresponding cracked blade, with a crack at the blade root. The lowest natural frequency at $\bar{\omega}_1 = 3{\cdot}476$ is the localization frequency. Figure 9 displays the effect of rotational speed on the frequency response of the cracked blade in this mistuned system, which reveals that the rotational speed is a significant factor for mode localization. The mode localization phenomenon is enhanced significantly with increase in the rotational speed.

4. CONCLUSIONS

The effects of crack on mode localization in the rotating blade-disk system have been studied. The major conclusions that can be drawn from this study are summarized as follows:

(1) It has been found that the crack on a bladed is one of the parameters for localization in the shrouded blade-disk system. For a coupled blade system, the existence of a crack may change the vibrational mode drastically, i.e., from the extended to the localized.

(2) The rotational speed has a significant influence on mode localization in the mistuned system. As the rotational speed of the disk is increased, the mode localization phenomenon is enhanced.

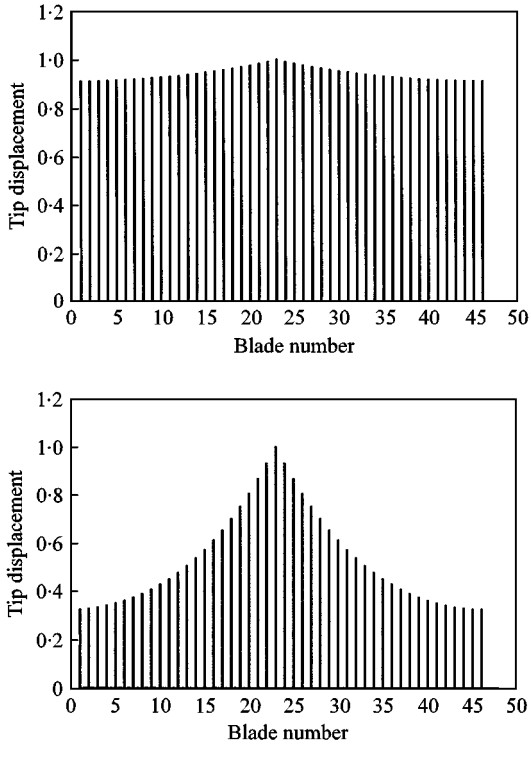

Figure 6. Tip displacements of the cracked system with strong modal coupling stiffness (for the 1st and 2nd order modes), $\gamma = 0{\cdot}05$, $\bar{L}_c = 0{\cdot}0$, $\bar{R}_c = 1{\cdot}0$, $\bar{\beta} = 10{\cdot}0$, $\bar{\Omega}/\bar{\omega}_1^* = 0{\cdot}5$, $\bar{\omega}_1^* = 3{\cdot}516$: (a) the first order mode ($\bar{\omega}_1 = 3{\cdot}549$); (b) the second order mode ($\bar{\omega}_{47} = 22{\cdot}085$).

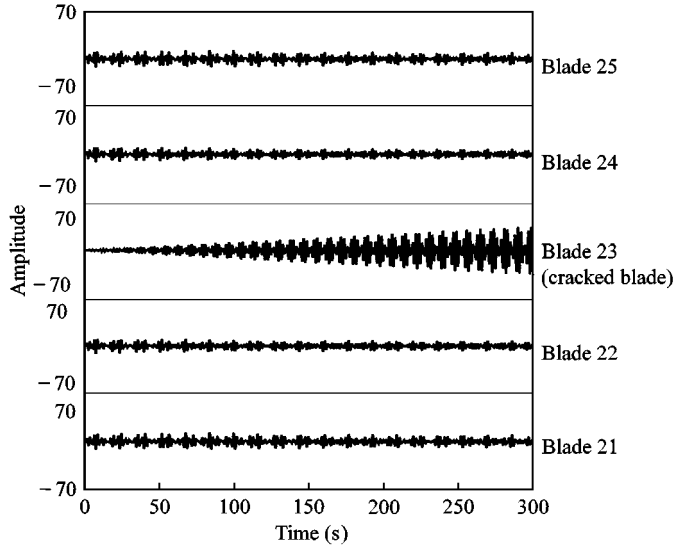

Figure 7. Tip responses of the blades under the lowest localization frequency $\bar{\omega}_1 = 5{\cdot}329$; $\gamma = 0{\cdot}01$, $\bar{L}_c = 0{\cdot}0$, $\bar{R}_c = 0{\cdot}2$, $\bar{\beta} = 0{\cdot}2$, $\bar{\Omega}/\bar{\omega}_1^* = 0{\cdot}5$.

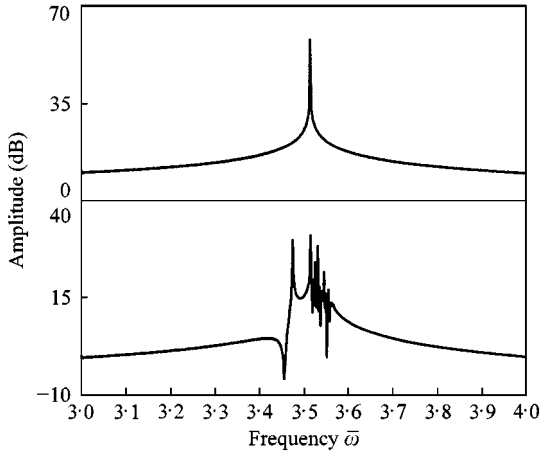

Figure 8. Difference between frequency responses of the 23rd blade with and without a crack, $\bar{\beta} = 0{\cdot}2$, $\bar{R}_c = 0{\cdot}5$, $\bar{\Omega}/\bar{\omega}_1^* = 0{\cdot}0$, $\bar{L}_c = 0{\cdot}0$: (a) $\gamma = 0{\cdot}0$; (b) $\gamma = 0{\cdot}1$.

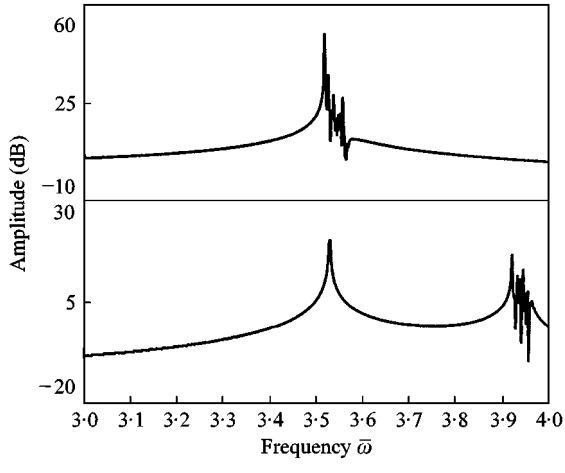

Figure 9. Frequency response vibration of the cracked blade with or without considering the rotating speed, $\bar{\beta} = 0{\cdot}2$, $\bar{R}_c = 0{\cdot}5$, $\bar{L}_c = 0{\cdot}0$, $\gamma = 0{\cdot}01$: (a) $\bar{\Omega}/\bar{\omega}_1^* = 0{\cdot}0$, (b) $\bar{\Omega}/\bar{\omega}_1^* = 0{\cdot}5$.

(3) The magnitude and location of the crack on the blade also affect mode localization in the shrouded blade-disk system.

(4) Only the cracked blade of the mistuned system shows a significant resonant response as the excitation frequency approaches the localization frequency. Obvious beat response on blades near the cracked blade is observed at localization frequency.

ACKNOWLEDGMENTS

The authors would like to acknowledge the support of the National Science Council, R.O.C., through grant no. NSC84-2212-E110–007.

REFERENCES

1. H. L. Bernstein and J. M. Allen 1992 *Transactions of the American Society of Mechanical Engineers, Journal of Engineering for Gas Turbines and Power* **114**, 293–301. Analysis of cracked gas turbine blades.
2. J. R. Galvele 1990 *Corrsion Science* **30**, 955–958. Surface mobility–stress corrsion cracking mechanism of steels for steam turbine rotor.
3. M. Krawczuk and W. M. Ostachowicz 1993 *Transactions of the American Society of Mechanical Engineers, Journal of Vibration and Acoustics* **115**, 524–528. Transverse natural vibrations of a cracked beam loaded with a constant axial force.
4. C. A. Papadopoulos and A. D. Dimarogonas 1988 *Transactions of the American Society of Mechanical Engineers, Journal of Vibration and Acoustics, Stress and Reliability in Design* **110**, 356–359. Stability of cracked rotors in the coupled vibration mode.
5. M. C. Wu and S. C. Huang 1997 *Proceedings of Design Engineering Technical Conferences, Computers in Engineering Conference, and Engineering Information Management Symposium, ASME Paper No. DETC/VIB*-4064, *Sacramento, California, USA*. Modal analysis of a rotating shaft–disk–blades system with a cracked blade.
6. L. Chen and C. Chen 1988 *Computers and Structures* **28**, 67–74. Vibration and stability of cracked thick rotating blade.
7. L. Chen and C. Chen 1993 *Computers and Structures* **46**, 133–140. Vibrational analyses of cracked pre-twisted blades.
8. B. Grabowski 1980 *Transactions of the American Society of Mechanical Engineers, Journal of Mechanic Design* **102**, 140–146. The vibrational behavior of a turbine rotor containing a transverse crack.
9. P. F. Rizos, N. Aspragathos and A. D. Dimarogonas 1990 *Journal of Sound and Vibration* **138**, 381–388. Identification of crack location and magnitude in a cantilever beam from the vibration mode.
10. O. O. Bendiksen 1987 *American Institute of Aeronautics and Astronautics Journal* **25**, 1241–1248. Mode localization phenomena in large spaced structures.
11. C. H. Hodges 1982 *Journal of Sound and Vibration* **82**, 411–424. Confinement of vibration by structural irregularity.
12. C. Pierre and E. H. Dowell 1987 *Journal of Sound and Vibration* **114**, 549–564. Localization of vibrations by structural irregularity.
13. S. T. We and C. Pierre 1988 *Transactions of the American Society of Mechanical Engineers, Journal of Vibration, Acoustics, Stress, and Reliability in Design* **110**, 429–438. Localization phenomena in mistuned assemblies with cyclic symmetry Part I: free vibrations.
14. S. T. We and C. Pierre 1988 *Transactions of the American Society of Mechanical Engineers, Journal of Vibration, Acoustics, Stress, and Reliability in Design* **110**, 439–449. Localization phenomena in mistuned assemblies with cyclic symmetry Part II: free vibrations.
15. C. W. Cai, Y. K. Cheung and H. C. Chen 1995 *Transactions of the American Society of Mechanical Engineers, Journal of Applied Mechanics* **62**, 141–149. Mode localization phenomena in nearly periodic systems.
16. C. W. Cai, H. C. Chen and Y. K. Cheung 1997 *Transactions of the American Society of Mechanical Engineers, Journal of Applied Mechanics* **64**, 940–945. Localization modes in periodic system with nonlinear disorders.
17. D. J. Cottney and D. J. Ewins 1974 *Transactions of the American Society of Mechanical Engineers, Journal of Engineering for Industry* **96B**, 1054–1059. Towards the efficient vibration analysis of shrouded bladed disk assemblies.
18. O. O. Bendiksen 1984 *Transactions of the American Society of Mechanical Engineers, Journal of Engineering for Gas Turbines and Power* **106**, 25–23. Flutter of mistuned turbo machinery rotors.

19. D. Afolabi 1985 *Vibrations of Blades and Bladed Disk Assemblies, Proceedings of the Tenth Biennial Conference on Mechanical Vibration and Noise, Cincinnati, Ohio, USA.* The frequency response of mistuned bladed disk assemblies.
20. D. Afolabi 1985 *Vibrations of Blades and Bladed Disk Assemblies, Proceedings of the Tenth Biennial Conference on Mechanical Vibration and Noise, Cincinnati, Ohio, USA.* The eigenvalue spectrum of mistuned bladed disk.
21. P. Basu and J. H. Griffin 1985 *Vibrations of Blades and Bladed Disk Assemblies, Proceedings of the Tenth Biennial Conference on Mechanical Vibration and Noise, Cincinnati, Ohio, USA.* The effect of limiting aerodynamic and structural coupling in models of mistuned blade disk vibration.
22. P. D. Cha and C. Pierre 1991 *Transactions of the American Society of Mechanical Engineers, Journal of Applied Mechanics* **58**, 1072–1081. Vibration of localization by disorder in assemblies of monocoupled, multimode component systems.
23. C. O. Orgun and B. H. Tongue 1994 *Transactions of the American Society of Mechanical Engineers, Journal of Vibration, Acoustics* **116**, 286–294. Mode localization in coupled circular plates.
24. C. Pierre and P. D. Cha 1989 *American Institute of Aeronautics and Astronautics Journal* **27**, 227–241. Strong mode localization in nearly periodic disordered structures.
25. C. Pierre 1990 *Journal of Sound and Vibration* **139**, 111–132. Weak and strong vibration localization in disordered structures: a statistical investigation.
26. J. H. Kuang and B. W. Huang 1997 *Proceedings of Design Engineering Technical Conferences, Computers in Engineering Conference, and Engineering Information Management Symposium, ASME Paper No. DETC/VIB-4391/4065, Sacramento, California, USA.* Corriolis effect on mode localization of a rotating bladed disk.
27. D. Broek 1986 *Elementary Engineering Fracture Mechanics*, 115–128: Dordrecht; Martinus Nijhoff Publishers.
28. H. Tada, P. Paris and G. Irwin 1973 *The Stress Analysis of Crack Handbook, Hellertown*, 2.13–2.14. Pennsylvania: del Research Corporation.